

# **Cost and efficiency considerations in On-board Chargers**

Marija Jankovic, Christian Felgemacher, Kevin Lenz, Aly Mashaly, Abdelmouneim Charkaoui  
ROHM SEMICONDUCTOR GMBH  
Karl-Arnold-Straße 15, 47877 Willich, Germany  
Tel.: +49 / (0) – 71172723722  
E-Mail: marija.jankovic@de.rohmeurope.com  
URL: <http://www.rohm.com>

## **Keywords**

Silicon Carbide (SiC), Efficiency, Automotive application, Battery charger, MOSFET, IGBT, Diode.

## **Abstract**

Silicon Carbide (SiC) is an enabling technology for highly efficient power train applications such as traction inverters and on-board chargers (OBC). SiC is foreseen as a dominating power device technology in premium vehicles. However, in compact electric and hybrid vehicles a market share with Silicon is also expected – setting high demands regarding efficiency and cost.

## **Introduction**

Very tight regulations for CO<sub>2</sub> emissions are being introduced in many countries worldwide, driving the development of electric and hybrid vehicles, that fully or partially use battery power and electric motors for traction. Penetration of hybrid and electric vehicles (EVs) is tightly coupled with the development of battery charging solutions. On the infrastructure side, the AC chargers developed first, providing a single- or three-phase grid connection to the car and relying on AC/DC conversion taking place inside the vehicle, in the on-board-charger (OBC). In this way, the charging power and the efficiency of charging is limited by the OBC size and capability. Typical OBCs support 3.6 – 7.2 kW single-phase charging and/or 11 – 22 kW three-phase charging. With the increase of the battery capacity inside the vehicles, especially in full EVs, AC charging became too slow leading first to an increase of OBC power rating, but later to the development of the DC chargers, capable of providing DC power to the car. DC charging power and efficiency is defined with the infrastructure installed power electronics and EV battery characteristics. Typical DC charging power ranges from 50 to 300 kW. DC charging therefore provides a reduction of charging time from a few hours to the portion of an hour, resulting in a trend of reducing the OBC power rating. Reducing weight, volume, and cost of an OBC and indirectly of an EV is an attractive trend for car manufacturers. Regardless of the power rating there is a trend of increasing the OBC power density, from 2 kW/l typically achieved with Si switches to 4-6 kW/l possible only with use of Wide-bandgap semiconductors [1, 2].

There are multiple reviews on OBC charging topologies and architectures [3,4]. The bidirectionality of OBC also appears as a trend, especially with the development of smart homes and concepts such as vehicle to grid (V2G), vehicle to vehicle (V2V) or vehicle to battery (V2B). The bidirectional concepts are also analyzed in literature [3]. Since the OBC should be able to work with both single- and three-phase grid, there are two main architecture concepts, modular and centralized, as presented in Fig. 1.

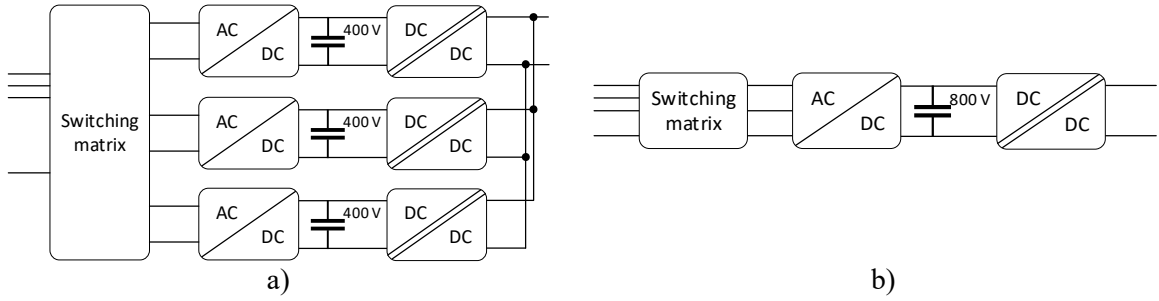


Fig. 1: Three-phase OBC Architecture concepts: a) Modular and b) Centralized.

Modular solutions use three identical blocks suitable for single-phase operation, typically rated at 3.6 kW or 7.2 kW each. These solutions allow the OBC manufacturers to have one-for-all solution blocks covering hybrid vehicles with only single-phase charging capability and EVs with both 3-phase and 1-phase charging capability.

On the other hand, centralized architectures use three phase AC/DC stages resulting in a higher DC link voltage and requiring 1200 V blocking voltage capability for the power semiconductors. This limits the choice on SiC-MOSFETs and Schottky barrier diodes and Si-IGBTs. Tight efficiency criteria and limited space usually limit the choice in this case to SiC. Centralized solutions require special strategies to enable single-phase operation. Sometimes this means that additional semiconductor components are added to the standard 3-phase PFCs.

This paper will first address the topologies and semiconductor technologies suitable for Modular and Centralized OBC architectures. Then it will discuss the simulation of 11 kW OBCs suitable for the European 3-phase 400 V Grid system based on the three most used topologies for two cases: predominantly SiC based solutions and predominantly Si based solutions. Finally, the AC/DC stage of a Modular solution suitable for a 3.6 kW 230 V phase to neutral grid voltage is investigated in more detail to assess the optimization of efficiency and cost. In this case the reduction of AC choke size can be achieved by using low switching losses devices and high switching frequencies. A compromise between the efficiency, semiconductor cost and AC choke could lie in the use of Hybrid IGBT which is addressed in the paper.

## Topology and technology benchmark

Based on Fig. 1 various topologies can be considered a in the AC/DC and DC/DC stages. Modular solutions allow multiple choices of semiconductor technologies, since AC/DC stages and the primary side of a DC/DC stage need 650 V blocking voltage capability, which could be realized with SiC MOSFETs or Gallium Nitride (GaN) transistors as well as with Silicon technology, such as SJ-MOSFETs and Si-IGBTs. A first trend in OBC was to use a Boost PFC as a single-phase AC/DC stage and an LLC as a DC/DC stage. This topology normally requires a Si diode bridge and 650 V Si MOSFET (such as SJ-MOSFET) and FRD. Further trend towards higher efficiency and miniaturization, involved utilizing the SiC SBD as a Boost diode and interleaving. Although simple, this topology has limited efficiency and it is being replaced with other single-phase topologies such as the Totem pole topology. This topology is especially interesting when employing Wide-bandgap semiconductors. Suitable DC/DC stage topology, used in modular architecture is typically unidirectional LLC realized with a half- or full-bridge primary. Secondary side semiconductors are always rated according to the battery voltage.

Centralized topologies require blocking of 800 V DC link voltage, which results in deployment of 1200 V semiconductors for full voltage blocking or 650 V semiconductors if 3-level topologies manage the DC link splitting. 2-Level solutions use a 3-phase full bridge as an AC/DC stage and isolated DC/DC stage with 800 V input. In the case of both AC/DC stage and primary side of DC/DC stage 1200 V semiconductors are used. High efficiency requirements and miniaturization trends lead to the selection of SiC MOSFETs since IGBTs are too slow and lossy, especially for high resonant frequency LLC converters. If a 3-level AC/DC stage is used, the DC link is divided into two halves, ensuring lower blocking voltage of some semiconductors in AC/DC stage, and also allowing the use of

two DC/DC stages, each with 400 V input. One popular AC/DC stage topology is Vienna rectifier, that requires 1200 V diodes and 650 V switches. Although perfectly suited for SiC semiconductors, it can deploy SJ-MOSFETs or GaN transistors as 650 V devices. Similarly, the primary side LLC switches can be realized with SiC, GaN or Si. One example of a GaN based Vienna rectifier with the split DC link for multiple DC/DC converters is presented in [1]. This topology features high efficiency with relatively low cost. Unlike the 2-level full bridge topology, which is bidirectional, the Vienna rectifier is unidirectional and has only limited P, Q power controllability [5]. Given that some car manufacturers often specify P, Q controllability and bidirectionality Vienna rectifiers require additional active semiconductors to support this, resulting in increased cost.

## Simulation – 11 kW OBC

A simulation study in PLECS has been performed to investigate the performance of different topologies and compare the solutions based on Si and SiC semiconductors for 11 kW unidirectional OBC feeding 800 V battery voltage. The semiconductors and switching frequency are selected in a way that their average junction temperature is less than 130 °C when case temperature is assumed to be 80 °C. Those thermal conditions correspond to typical coolant temperatures of 60 °C and good thermal contact case to coolant. Additionally, enough buffer to the datasheet defined maximum junction temperatures is ensured. The loss and thermal models are constructed based on the datasheets. The battery voltage varies between 600 V (empty battery) and 850 V (full battery) and the charging power is assumed to be 11 kW, since this is the case during 80 % of the charging time.

Three different topologies as shown in Fig. 2 are compared: 2-level based on full bridge and LLC, 3-level based on Vienna rectifier and LLC and single-phase solution, suitable for the modular architecture, based on Totem Pole and single-phase LLC. The target was to achieve an efficiency of above 96 % for all operating points.

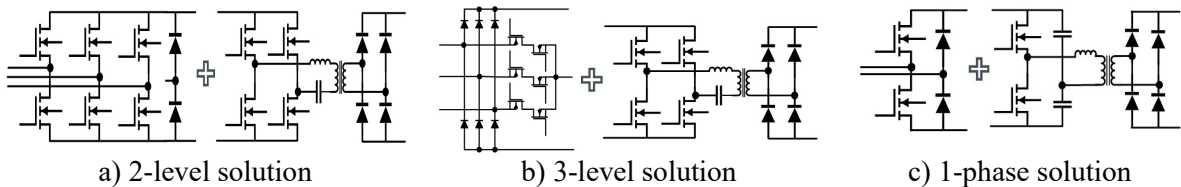


Fig. 2: Different OBC topologies: a) 2-level, b) 3-level and c) 1-phase solution suitable for modular architecture. DC link and AC side inductor are not presented here, but they are part of the design.

All three topologies are simulated based on SiC components, such as MOSFETs and Schottky barrier diodes, except for low frequency switched devices such as diodes in Totem pole (Fig. 2 a) and c)). Additionally, all three topologies are simulated based on Si devices, such as Si IGBTs and SJ-MOSFETs, where use of Si devices would not significantly compromise efficiency and SiC devices where Si device would significantly reduce efficiency. As an example, topology from Fig. 2. a) used Si IGBT at the PFC stage and SiC in LLC stage; topology from Fig. 2. b) uses only SiC diode in Vienna rectifier and all other components are based on Si, thanks to the use of split DC link and two 400 V input LLCs; topology from Fig. 2. c) is fully based on Si. The obtained efficiency profiles, in the 3-phase full power operating point are presented in Fig. 3 a). In those profiles only semiconductor losses obtained by simulation are considered.

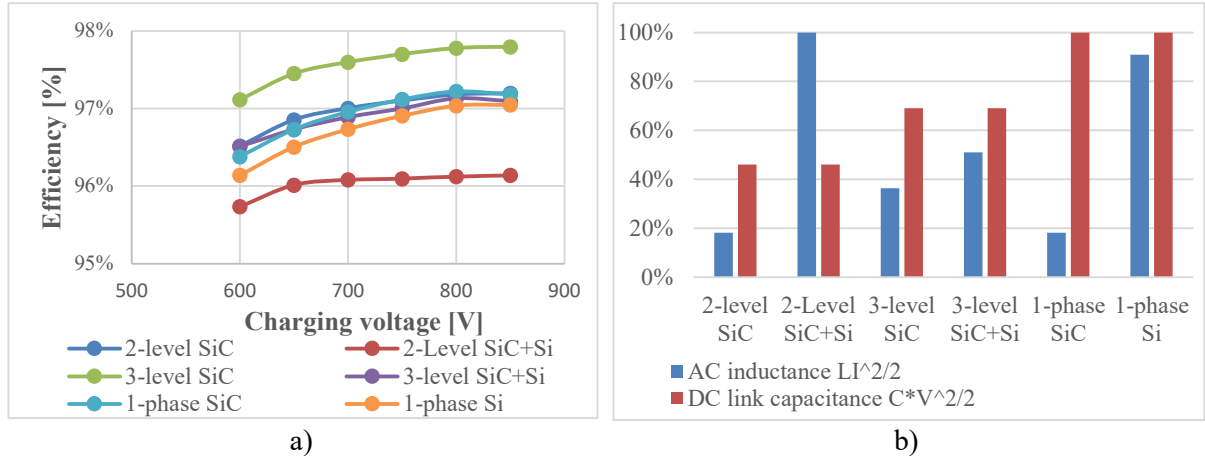


Fig. 3: Comparison of the 3 simulated solutions based on SiC and Si a) Efficiency vs. charging voltage; b) Normalized energy stored in AC inductance and DC link capacitance.

The 3-Level solution based on SiC has the highest efficiency due to the very efficient Vienna rectifier. The 2-level solution based on SiC, the single-phase solution based on SiC and the 3-level solutions based on either SiC or Si have similar efficiency profiles. Their efficiency peaks above 97 %. The Single-phase solution based on Si has only slightly lower efficiency than its SiC counterpart. The 2-Level solution based on SiC and Si that uses IGBTs in the PFC stage has more than 1 % lower efficiency than its SiC counterpart. This result indicates that in the case of 3-level solutions or single-phase solutions, Si devices could also lead to high efficiency operation.

Fig. 3. b) shows the normalized energy stored in the AC inductances and DC link capacitances. In this comparison a value of 100 % corresponds to the highest energy stored in AC inductance and DC link capacitance, respectively. For AC inductance we can see that the highest energy stored is in 2-level SiC+Si based solutions, whereas the highest energy stored in DC link capacitance is in 1-phase solutions suitable for modular architecture. The 2-Level SiC based solution has the lowest energy stored in AC inductances and DC link capacitances, and therefore lowest cost of those elements. 3-Level based solutions have moderate energy stored in AC inductances and DC link capacitances. Single-phase solutions store high energy in DC link capacitances. Although the efficiency of the Si based single-phase solution, considering semiconductor losses, is relatively high, this solution shows very high energy stored in AC inductance which might lead to the higher overall losses. The DC capacitances have significant volume in an OBC [6], and therefore where 3-phase OBC is implemented and OBC volume is critical, the use of centralized architecture and 2- or 3-level solutions might be preferred.

## Modular OBC with Totem Pole topology

The Totem Pole topology, presented in Fig. 4. a), is very promising for modular OBC designs, since it features high efficiency, possibility for interleaved design and upgrade to a bidirectional solution. One example of 7.2 kW bidirectional OBC based on Totem Pole topology is presented in [2]. Switches Q1 and Q2 are fast switched, whereas the diodes D1 and D2 switch at 50 Hz. In general, use of Wide-bandgap devices guarantees high efficiency with high switching frequency, being in the range of hundreds of kHz for GaN and around 100 - 150 kHz for SiC. Use of Wide-bandgap devices means increase of semiconductor costs and decrease of the size and cost of passive elements. Given the single-phase nature of Totem Pole topology, the current and voltage on the DC link side is highly dominated by 100 Hz ripple, as presented in Fig. 4. b) requiring large DC link capacitances, typically realized with electrolytic capacitances. The capacitor bank is rated according to this ripple and therefore not significantly influenced by switching frequency. There are techniques of limiting the DC link capacitor bank such as active power decoupling, by adding additional circuit components [7]. However, [2] suggests that minimization of power density and volume is provided by proper arrangement of electrolytic capacitances and magnetic elements. Similar approach is done in the experimental converter presented in this paper. Switching frequency influences AC inductor sizing and therefore using the devices with lower switching losses, contributes to the OBC miniaturization.

Replacing the diodes D1 and D2 with Si MOSFETs used in synchronous rectification mode reduces the losses in 50 Hz operated leg and provides bidirectionality. In this paper we will focus on fast switching devices in a Totem pole topology (Q1 and Q2) and look how different semiconductor technologies influence efficiency and switching frequency.

A Hybrid IGBT, the name is used here for a discrete device comprising of a Si-IGBT and a co-packed SiC Schottky barrier diode, could be a compromise for AC inductor size vs. semiconductor cost in a Totem pole topology. The performance of hybrid IGBT, standard Si-IGBT with co-packed Si Diode and SiC MOSFET based solutions are compared in Totem pole topology.

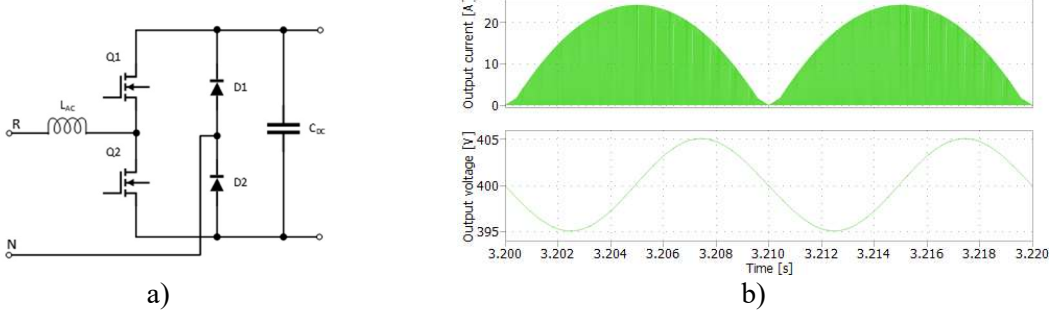


Fig. 4: a) Totem Pole topology and b) Typical current and voltage at the output.

## Simulation based on Experimental evaluation – 3.6 kW Totem Pole

The simulation of a 3.6 kW Totem pole converter with 400 V output and 230 V single-phase grid has been performed. This is a typical power rating of a single phase OBC suitable of 3.6 kW single- and 11 kW three-phase charging. The same solution can be used in 7.2 kW single-phase charger by using two equivalent building blocks. Losses in the high frequency leg of a Totem pole are compared for different semiconductor components. Two different 30 A 650 V IGBT's are compared together with one SiC MOSFET. Both IGBT devices are based on the same IGBT die and different antiparallel diodes: 25 A Si diode (RGW60TS65DHR) and 25 A SiC diode (RGW60TS65CHR) [8, 9]. The IGBTs with antiparallel diodes are packed in TO-247-3L packages. SiC device is 45 mΩ 750 V MOSFET SCT4045DRHR packed in TO-247-4L [10]. TO-247-4L provides better switching characteristics compared to TO-247-3L package.

All three devices are firstly evaluated in the double-pulse test (DPT) experimental setup. This setup has a possibility to capture switching waveforms of the actively switched and commutating device in a half-bridge. DC link voltage is kept constant, and current is varied. DPT test is performed at 25 °C, 100 °C and 150 °C. Comparison of turn on and turn off behavior of all three devices is compared in Fig. 5 at 100 °C, 400 V DC link and 18 A. The turn on behavior (Fig. 5. a) shows a significant difference between the current overshoot and therefore turn on losses and diode reverse recovery losses by standard and hybrid IGBT (Fig. 6). The SiC MOSFET turns faster on than the IGBT devices. Fig. 5. b) shows significant difference in turn off speed of IGBT devices and SiC MOSFET. IGBT devices have significant tail current that amounts to high turn off losses.

Fig. 6 presents turn-on losses and reverse recovery losses (switching energies) calculated from transients captured by DPT at 100 °C. This highlights the main difference between standard IGBT co-packed with Si diode and Hybrid IGBT co-packed with SiC diode.

DPT test is performed at 25 °C, 100 °C and 150 °C to provide enough data for switching loss model in Plecs simulation environment. Inputs for the simulation model are switching energies calculated from measurements, as presented in Fig. 6. Conduction losses are modelled based on the datasheet information at 25 °C and 175 °C and thermal impedance is modelled with a 3<sup>rd</sup> order Cauer model. Case temperature in all the cases is set to 80 °C assuming the high performant water cooling in the automotive environment.

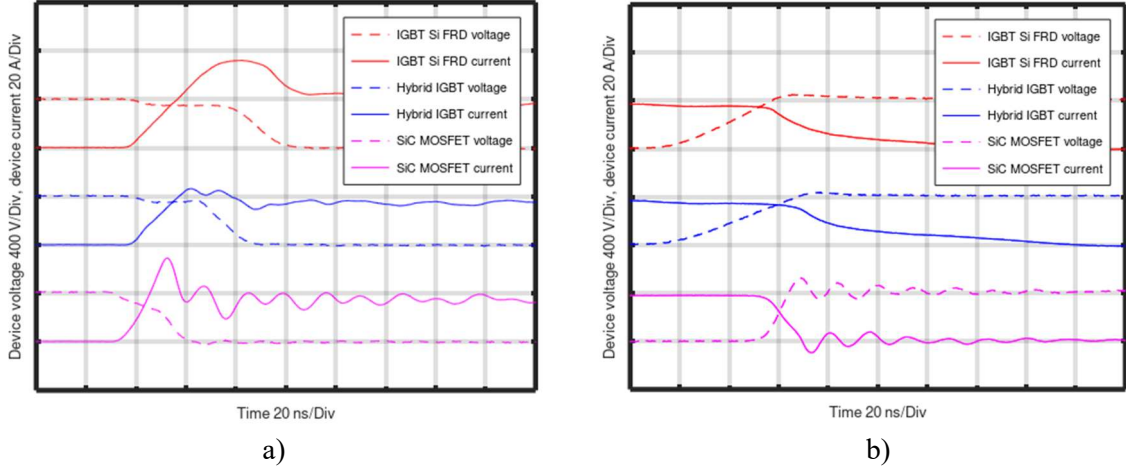


Fig. 5: Comparison of switching behavior by a) turn on and b) turn off. In the case of both IGBT devices driving condition is given with 15 V/0 V,  $R_{G\_on} = R_{G\_off} = 10 \Omega$ . SiC MOSFET has driving condition of 18 V/0 V,  $R_{G\_on} = 10 \Omega$  and  $R_{G\_off} = 3.3 \Omega$ .

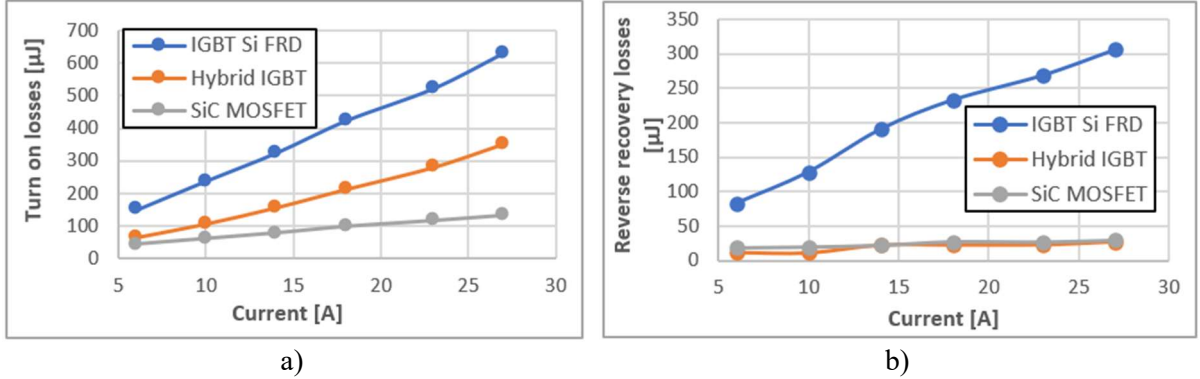


Fig. 6: Comparison of switching losses by a) turn on and b) reverse recovery. In the case of both IGBT devices driving condition is given with 15 V/0 V,  $R_{G\_on} = R_{G\_off} = 10 \Omega$ . SiC MOSFET has driving condition of 18 V/0 V,  $R_{G\_on} = 10 \Omega$  and  $R_{G\_off} = 3.3 \Omega$ .

Fig. 7. a) shows the semiconductor losses (both switching and conduction losses) in the switching leg normalized with the rated power at rated power operation. Unlike standard IGBT with Si diode, hybrid IGBT allows switching frequencies up to 90 kHz. Hybrid IGBT solution at 90 kHz and nominal power has 1 % less efficiency than the SiC MOSFET switched with the same switching frequency.

Fig. 7. b) shows normalized system parameters in three selected cases of switches: IGBT switched at 40 kHz, Hybrid IGBT switched at 60 kHz and SiC MOSFET switched at 100 kHz. Normalized system parameters are given as a percentage of the maximum of each parameter for all three cases (standard IGBT, Hybrid IGBT and SiC MOSFET). AC choke is selected to ensure 20 % peak-to-peak AC current ripple. As seen from the Fig. 7. b) SiC MOSFET based solution requires only 40 % and Hybrid IGBT 70 % of the AC choke inductance required in the case of standard IGBT based solution. Reduction of the inductance means reduction of stored energy and choke size, cost and weight and additionally reduction of losses in the AC choke. However, further increase of the switching frequency does not significantly reduce the required inductance value. For the selected switching frequencies and rated power operation, the losses in the switching leg of the Totem pole in a IGBT and Hybrid IGBT case are comparable. Losses in the switching leg bases on SiC MOSFET are 40 % lower, which results in 0.56 % higher system efficiency at nominal power. Finally, price of those switches is compared based on the internal price database. IGBT with Si diode costs approximately one third of SiC MOSFET price whereas expected Hybrid IGBT price development is between standard IGBT and SiC MOSFET price.

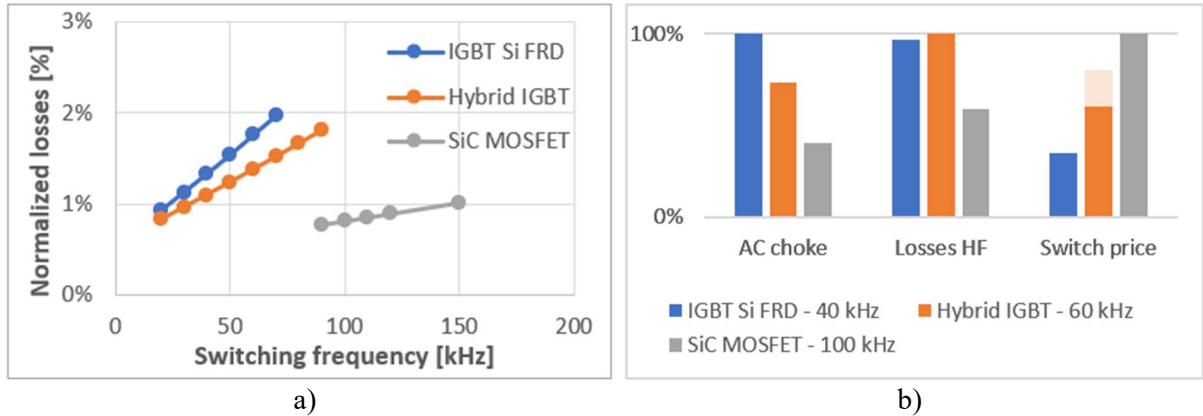


Fig. 7: a) Normalized switching losses in the switching leg at rated power operation and b) Normalized system parameters at the selected switching frequency: required AC choke for 20 % current ripple, losses in the switching leg and switch price.

The above analysis concludes the highest efficiency of SiC based Totem Pole even with the significantly higher switching frequency. Higher efficiency leads to reduction of cooling requirements which could lead to cost savings. Related to the cost targets, SiC MOSFET has the highest price but therefore the smallest AC choke. The size of the AC choke in the case of standard IGBT might not fit to OBC volume and weight requirements, and its price might compensate for the low semiconductor cost. Hybrid IGBT is an intermediate solution in both semiconductor price and choke size and cost. This analysis does not consider the EMI filtering size which would be briefly discussed in the next chapter.

## Experimental results based on 45 mΩ 750 V SiC MOSFET Totem Pole

Experimental verification of a Totem Pole converter based on the 45 mΩ 750 V SiC MOSFET from the previous chapter has been performed to evaluate system efficiency. The experimental converter is bidirectional using Si SJ-MOSFET in synchronous rectification mode instead of the diodes in Fig. 4. a). Converter parameters are presented in Table I. The control algorithm consists of two control loops, slower proportional-integral controller of DC voltage and inner fast proportional-resonant AC current controller.

**Table I: Converter parameters**

Vin	Vout	Power	L <sub>AC</sub>	f <sub>sw</sub>	C <sub>DC</sub>
230 V	400 V	3.4 kW	185 μH	100 kHz	2.24 mF

Fig 8. shows the photograph of the Totem Pole converter. In this case simple heatsink air cooling is used and therefore the converter is operated at somewhat higher case temperatures than in typical OBC application. As it can be seen, significant volume belongs to DC link capacitors that are independent on switching frequency, AC choke and EMI filters. AC choke is in this case minimized thanks to the 100 kHz switching frequency. AC side EMI filter has two stages as shown on Fig. 8. Use of Si switch technology would increase the size of the AC choke but might reduce the size of EMI filter. EMI filter design of the Totem Pole converter for all cases analyzed in the previous chapter is outside the scope of this paper.

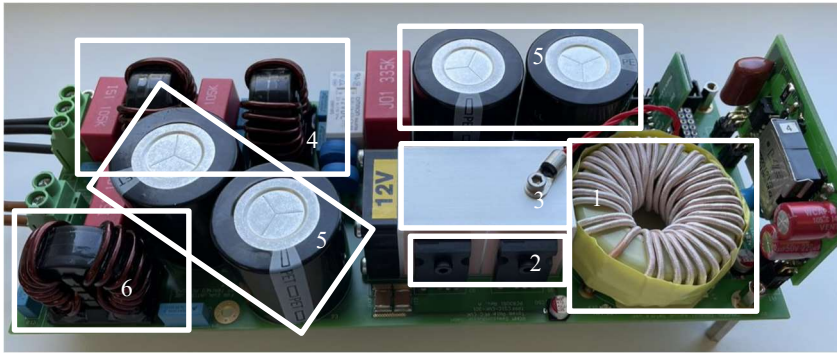


Fig. 8: Experimental Totem Pole converter.

Fig. 9 shows the efficiency behavior from input power source to the output including the control electronics, such as auxiliary power supply, and cooling fan. As shown the obtained efficiency of the overall system is higher than 98 % at the nominal power. The measured case temperature of the switching leg MOSFETs is about 110 °C which is 30 °C higher than in the case of simulation study. This would result in slightly higher losses compared to estimated 0.8 % at 100 kHz. However, considering that the overall system efficiency is higher than 98 % and there are losses associated with low frequency leg, traces, filters and control electronics, the obtained results match well high SiC based solution efficiency. Using a Hybrid IGBT would in this case mean reducing the switching frequency to 60 kHz, increasing AC choke (cost and volume), possibly reducing AC side EMI filtering, and reducing efficiency by roughly 0.6 % at the nominal power.

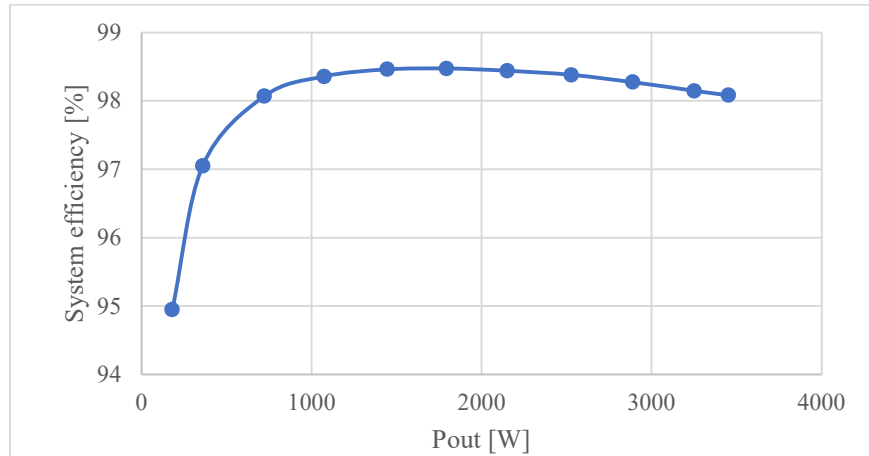


Fig. 9: Power analyzer obtained overall system efficiency of the experimental 3.4 kW Totem pole and 400 V output voltage.

## Conclusion

This paper is a review of the current trends in OBC application, covering the topology and semiconductor technology trends. Centralized and modular architecture have been discussed together with the relevant topologies and selection of suitable semiconductors for those topologies. Three different topologies have been simulated to assess the efficiency and passive components sizing. Centralized 3-level Vienna based solution has the highest efficiency especially when based on SiC semiconductors. SiC based 2-level topology has the lowest requirement of passive elements providing the miniaturization of the system. Additionally, it features full P, Q controllability on the AC side, which makes it suitable for bidirectional solutions required for V2G/V2V/V2B trends. Therefore, SiC is the suitable choice for centralized OBC architecture, and it could be combined with Si in 3-level solutions.

Among Si based solutions, single-phase solution suitable for modular architecture has high efficiency based on Si but therefore the highest requirement for passive elements.

The second part of the paper discusses Totem pole, as an AC/DC stage of a single-phase solution suitable for modular architectures. This part focuses on the reduction of the AC choke by using a Hybrid IGBT with a co-packed SiC diode instead of a standard IGBT with Si diode. In Totem pole the highest efficiency, highest switching frequency and the smallest required AC choke is guaranteed with SiC MOSFET. Cost of a SiC MOSFET is higher than the cost of Si devices and the optimal solution depends on a trade off between cost, efficiency, and volume. Use of SiC MOSFET, on the other hand, reduces the cost of passive elements and cooling. However, Hybrid IGBT (IGBT with co-packaged SiC diode) could be suitable for more cost optimized solutions.

Finally, SiC based Totem pole converter has been built using 45 mΩ SiC MOSFETs in the fast switching leg. The experimental converter operated at 100 kHz confirmed high efficiency of above 98 % at the nominal power. The system design is very compact although it has been designed with forced air cooling, instead of more effective water-cooling typically present in OBC applications.

## References

- [1] M. Kasper, J. Azurza, G. Debay, Y. Li, M. Heider, J. W. Kolar, "Next Generation GaN-based Architectures: From 240W USB-C Adapters to 11kW EV On-Board Chargers with Ultra-high-Power Density and Wide Output Voltage Range," 2022 IEEE Proceedings of the Conference on Power Electronics and Intelligent Motion (PCIM Europe 2022), Nuremberg, Germany, May 10-12, 2022.
- [2] F. Vollmeier, A. Connaughton, I. Recepi, T. Langbauer, M. Pajnic, W. Konrad and C. Mentin, "Tiny Power Box - Exploiting Multiport Series Resonant Topologies for Very High-Power Density Onboard Chargers," 2022 IEEE Proceedings of the Conference on Power Electronics and Intelligent Motion (PCIM Europe 2022), Nuremberg, Germany, May 10-12, 2022.
- [3] J. Yuan, L. Dorn-Gomba, A. D. Callegaro, J. Reimers and A. Emadi, "A Review of Bidirectional On-Board Chargers for Electric Vehicles," in IEEE Access, vol. 9, pp. 51501-51518, 2021, doi: 10.1109/ACCESS.2021.3069448
- [4] I. Subotic and E. Levi, "A review of single-phase on-board integrated battery charging topologies for electric vehicles," 2015 IEEE Workshop on Electrical Machines Design, Control and Diagnosis (WEMDCD), 2015, pp. 136-145, doi: 10.1109/WEMDCD.2015.7194522.
- [5] D. A. Molligoda, J. Pou, C. J. Gajanayake and A. K. Gupta, "Analysis of the Vienna Rectifier under Nonunity Power Factor Operation," 2018 Asian Conference on Energy, Power and Transportation Electrification (ACEPT), 2018, pp. 1-7, doi: 10.1109/ACEPT.2018.8610866.
- [6] Baek, J.; Park, M.-H.; Kim, T.; Youn, H.-S. Modified Power Factor Correction (PFC) Control and Printed Circuit Board (PCB) Design for High-Efficiency and High-Power Density On-Board Charger. *Energies* 2021, *14*, 605. <https://doi.org/10.3390/en14030605>
- [7] A. S. Morsy and P. N. Enjeti, "Comparison of Active Power Decoupling Methods for High-Power-Density Single-Phase Inverters Using Wide-Bandgap FETs for Google Little Box Challenge," in IEEE Journal of Emerging and Selected Topics in Power Electronics, vol. 4, no. 3, pp. 790-798, Sept. 2016, doi: 10.1109/JESTPE.2016.2573262.
- [8] [online] <https://fscdn.rohm.com/en/products/databook/datasheet/discrete/igbt/rgw60ts65dhr-e.pdf> access on 13.6.2022.
- [9] [online] <https://fscdn.rohm.com/en/products/databook/datasheet/discrete/igbt/rgw60ts65chr-e.pdf> access on 13.6.2022.
- [10] [online] <https://fscdn.rohm.com/en/products/databook/datasheet/discrete/sic/mosfet/sct4045drhr-e.pdf> access on 13.6.2022.